Attachment B

ANALYSIS OF NEUTRON FLUX LEVELS AND SURVEILLANCE CAPSULE LEAD FACTORS FOR THE INDIAN POINT UNIT 2 REACTOR USING A LOW LEAKAGE CORE

S. L. Anderson
Westinghouse Electric Corporation
Nuclear Technology Division
July 1982

SUMMARY

Calculations have been performed to evaluate the impact of an L^3P (Low Leakage Loading Pattern) on the fast neutron (E >1.0 Mev) exposure of the Indian Point Unit 2 pressure vessel as well as on the lead factors associated with each of the reactor vessel surveillance capsules. The fuel loading pattern to be installed during the current refueling outage was used as the basis for this evaluation. Results of this analysis indicate that the use of the L^3P effects a reduction of the peak neutron flux (E >1.0 Mev) at the pressure vessel inner radius from 1.8×10^{10} n/cm^2-sec to 1.0×10^{10} n/cm^2-sec. Coincident with this reduction in maximum neutron flux are changes in the capsule lead factors at both the 4° and the 40° azimuthal locations. At the 4° locations the lead factor is calculated to increase from 1.09 to 1.62 while at the 40° location a decrease from 3.72 to 3.48 is observed.

INTRODUCTION

Knowledge of the neutron environment within the pressure vessel-surveillance capsule geometry is required as an integral part of LWR pressure vessel surveillance programs for two reasons. First, in the interpretation of radiation induced properties changes observed in materials test specimens, the neutron environment to which the test specimens were exposed must be known. Second, in relating the changes observed in the test specimens to the condition of the reactor pressure vessel, a relationship between the environment at various positions within the reactor vessel and that experienced by the test specimens must be established. The former requirement is normally met by employing a combination of rigorous analytical techniques and measurements obtained with passive neutron flux monitors contained in each of the surveillance capsules. The latter information, on the other hand, is derived solely from analysis.

This report describes a discrete ordinates Sn transport analysis performed for the Indian Point Unit 2 reactor to determine the fast neutron (E>1.0Mev) flux levels within the reactor vessel and surveillance capsules; and, in turn, to develop lead factors for use in relating neutron exposure of the pressure vessel to that of the surveillance capsules. The current fuel cycle L^3P (Low Leakage Loading Pattern) was employed to derive the neutron source distribution within the reactor core. Results of this analysis are compared with prior calculations[5] which employed a design basis core power distribution based on an out-in loading scheme that utilized fresh fuel at all peripheral core locations.

METHOD OF ANALYSIS

In the analysis of the neutron environment within a PWR reactor geometry, predictions of the spatial neutron flux magnitude and energy spectra are made with the DOT[1] two-dimensional discrete ordinates transport code. First, the radial and azimuthal distributions are obtained from an R, θ computation normalized to the reactor core power density representative of the axial midplane. A second calculation in R, Z geometry is used to

provide relative axial variations of neutron flux in the pertinent regions of the pressure vessel. A three-dimensional description of the neutron environment is then constructed by assuming separability and using the relation

$$\phi\ (R, \Theta, Z, E) = \phi\ (R, \Theta, E)\ F\ (Z, E)$$

Where ϕ (R, θ, E) represents the absolute neutron flux magnitude at the core midplane as determined from the R, θ computation and F(Z, E) is the relative axial distribution obtained from the R, Z analysis and normalized to unity at the core midplane.

A plan view of the Indian Point Unit 2 reactor geometry is shown in Figure 1. Since the reactor exhibits 1/8 core symmetry, only a 0° -45° sector of the geometry at the core midplane is shown. In addition to the core, reactor internals, pressure vessel, and primary shield shown in Figure 1, eight irradiation capsules attached to the thermal shield are included in the 4 loop plant design to constitute the reactor vessel surveillance program. Four of these capsules are located symmetrically at 4° from a cardinal axis while the remaining four are positioned at a 40° azimuth, also referenced to a cardinal axis. The relative locations of these two sets of capsules are indicated by points A and B on Figure 1.

A plan view of a single surveillance capsule attached to the thermal shield is depicted in Figure 2. The stainless steel specimen container is one inch square and approximately 38 inches in length. The containers are positioned axially such that the specimens are centered on the core midplane, thus, spanning the central three feet of the twelve foot high reactor core.

From a neutronic standpoint, the inclusion of the surveillance capsule structures in the R, θ analytical model is significant. Neutron dosimetry from these capsules provides a means for evaluating the analytical model by direct comparison with measurement. Since the presence of the capsules has a marked impact on both the neutron flux magnitude and energy spectrum, a meaningful comparison of measurement and calculation

can be made only if these perturbation effects are properly accounted for in the analysis.

The geometry used in the R, Z analysis of the Indian Point Unit 2 reactor is shown schematically in Figure 3. In this case, the reactor core is treated as an equivalent volume cylinder of cross-sectional area equal to the actual core area. The axial extent of the geometry shown in Figure 3 is chosen such that all regions of the pressure vessel which are expected to experience significant radiation damage during the service life of the plant are included in the analysis. Due to their very limited azimuthal extent, the surveillance capsules themselves are not explicitly represented in the R, Z model.

The analysis of both the R, θ and R, Z models employs 21 neutron energy groups and a P1, Legendre polynominal expansion of the scattering cross-sections. These cross-sections are generated with the Westinghouse version of the GAMBIT[2] code system. Fine group to broad processing is carried out by the APPROPOS[3] and ANISN[4] codes with zone dependent spectra calculated with ANISN used as weighting functions. The final broad energy group structure is listed in Table 1.

In the R, θ analysis, the discretization of the angular flux is represented by a symmetric S_8 quadrature. However, in the R, Z case the use of this relatively low order quadrature set can often prove to be inadequate. At large depths within the pressure vessel the axial distribution of neutron flux is dominated by neutron streaming in the annulus between the pressure vessel wall and the primary biological shield. To account for this effect a high resolution angular quadrature is required. Therefore, in this analysis a 124 angle asymmetric quadrature is employed. For regions of the reactor which are above the core midplane, this quadrature is constructed with 109 angles biased in the upward directions, i.e., the direction of prime interest, and 15 angles biased downward. For analysis below the core midplane, the quadrature is reversed with 109 angles biased in the downward direction. Complete descriptions of both the symmetric S_8 and the asymmetric 124 angle quadratures are given in Reference 1.

The geometric modeling of the R, θ geometry shown in Figure 1 was accomplished with a spatial mesh array consisting of 106 radial by 94 theta mesh. In the R, Z case the modeling included 61 radial mesh and 116 axial mesh.

The neutron source used in the current calculation was based on the actual L^3P power distribution to be incorporated into the Indian Point Unit 2 fuel cycle during the upcoming refueling outage. Therefore, the results of this analysis represent a plant specific evaluation.

On the other hand, the design basis core power distributions used in the prior analysis were generic in nature. In the design basis analysis, limiting core power distributions applicable to long term operation were derived from a statistical analysis of calculated distributions from all available independent cycles of a given reactor type; i.e., 4-loop. These long term distributions represent an upper tolerance limit on the average BOC (beginning of cycle) and EOC (end of cycle) power in peripheral fuel assemblies based on a 95 percent probability with 95 percent confidence. These distributions are also biased to account for observed differences between calculated and measured power in the peripheral fuel assemblies. Rod by rod power distributions which provide spatial gradients within each of the peripheral assemblies are derived from typical equilibrium EOC calculations. These gradients are also biased to account for inadequacies in diffusion theory computations near the core boundaries. It should be noted that these design basis distributions were based solely on an out-in fuel management scheme; and, thus do not reflect any operation with L^3P cores.

A single time-averaged axial power distribution was used for long term application in all Westinghouse reactor models. This approach is supported by an investigation of time-varying axial power distributions expected in first core and reload fuel regions for base load operation. The results of this study indicate that differences in steady state fuel performance resulting from the use of time-varying vs. constant axial power distributions are negligible.

RESULTS OF ANALYSIS

Results of the neutron transport analysis of the Indian Point Unit 2 reactor are summarized in Figures 4 through 8 and in Tables 2 through 4. In all cases data is presented for both the L^3P and the design basis calculations.

In Figure 4, the calculated maximum fast neutron flux (E>1.0 Mev) levels at the pressure vessel inner radius are presented as a function of azimuthal angle. The impact of implementing the low leakage pattern is clearly evident.

In Figure 5, the calculated maximum fast neutron flux (E>1.0 Mev) is given as a function of radial position within the vessel wall for both the low leakage and the design basis configurations. The relative axial variation of neutron flux within the vessel is shown in Figure 6. Axial variations of absolute fast neutron (E>1.0 Mev) flux can be obtained using Figures 4, 5, and 6.

The neutron flux (E>1.0 Mev) distributions within the surveillance capsules are highlighted in Figures 7 and 8. Figure 7 depicts the azimuthal variation of fast neutron flux at a radius equal to that of the surveillance capsule centerline (R = 211.33). The perturbation introduced by the presence of the capsule material is clearly evident. In Figure 8, the radial gradient of neutron flux (E>1.0 Mev) at the azimuthal center of the capsules is depicted. It is of interest to note that from the core side of the test specimens to the pressure vessel side of the test specimens the fast neutron flux drops approximately 30%.

Lead factors for each of the Indian Point Unit 2 surveillance capsules are presented in Table 2. The lead factor is defined as

$$LF = \frac{\phi_C}{\phi_{PV}}$$

where: ϕ_C = neutron flux (E>1.0Mev) at the geometric center of the surveillance capsule

ϕ_{PV} = maximum neutron flux (E>1.0Mev) at the pressure vessel inner radius

In Table 3, the relative neutron flux spectra calculated to exist at the center of the surveillance capsules are listed. The data in each case have been normalized to a total neutron flux of 1 n/cm^2-sec. This spectral information may be used to develop spectrum averaged reaction cross-sections for use in analyzing neutron dosimeter packages contained within the surveillance capsules. A set of cross-sections in the group structure listed in Table 3 are given in Table 4 for selected fast neutron reactions. These data are based on information found in the ENDF IV dosimetry file.

ADEQUACY OF THE ANALYTICAL METHOD

The calculated fast neutron flux distributions depicted in Figures 4 through 6 may be used in conjunction with damage trend curves to predict the degree of embrittlement of the reactor vessel steel over its service life. The accuracy of these neutron flux profiles depends on the analyst's ability to define an appropriate core power distribution, the adequacy of the cross-sections used in the transport analysis, and the applicability of the geometric modeling of the reactor. Taken as a whole, these factors combine to yield an overall uncertainty in the prediction of neutron flux and fluence within the pressure vessel wall.

In order to assess the potential uncertainties in the neutron flux and fluence predictions, calculated results based on the methodology described herein are compared with measurements obtained from a number of operating PWR's. Neutron dosimetry results from a variety of plant reactor vessel surveillance programs provide a growing data base for use in verifying computer analyses. Data from this source have the advantage of extending over several reactor internals geometries as well as over many years of plant operation. A second and equally important set of data for use in methods evaluation comes from a series of measurements obtained in the annulus region between the pressure vessel and primary biological shield of two operating plants. Comparison of calculated neutron radiation levels with this data set provide confidence in the analytical results not only internal to the reactor, but through the pressure vessel thickness as well.

Comparisons of the calculated saturated activity of four common fast neutron detectors with measurements obtained from ten 2-loop and eight 4-loop reactor vessel surveillance capsules are depicted in Tables 5 and 6, respectively. For both plant types and for all four reactions the agreement between calculation and the average measured value is within ±10 percent. The variability in the measurements themselves on the other hand is characterized by maximum/minimum ratios ranging from 1.29 to 1.63 for 2-loop capsules and from 1.22 to 1.40 for the 4-loop data. These comparisons indicate that on the average the best estimate neutron transport calculation does an excellent job of predicting neutron radiation levels at the surveillance capsule locations. Furthermore, the best estimate computation with an uncertainty level of ±20 percent brackets all of the experimental data listed in Tables 5 and 6. It may also be noted that, since the flux monitors in Tables 5 and 6 respond over different portions of the neutron energy spectrum, the agreement between calculation and measurement implies that the neutron energy spectra as well as the neutron flux magnitude are being determined well by the analytical method.

Additional comparisons of calculations with measurements are shown in Table 7. As stated earlier, these data were obtained external to the pressure vessel in the air gap between the vessel and the primary shield. The data, representative of core midplane neutron flux levels, were obtained at 4 azimuthal locations external to a Westinghouse 3-loop reactor and at the single point characteristic of the maximum flux external to a 4-loop reactor. Again, the agreement between calculation and measurement is excellent with discrepancies falling in the ±15 - 20 percent range. These comparisons support the contention that the Westinghouse methodology can accurately predict fast neutron fluence gradients through the pressure vessel wall.

Although a rigorous statistical analysis of the available data has not been presented, there is sufficient information given in Tables 5 through 7 to support an uncertainty level of ±20 percent relative to the best estimate fast neutron (E >1.05 Mev) flux levels calculated with the Westinghouse methodology outlined in this report.

REFERENCES

1. Soltesz, R. G.,et al, "Nuclear Rocket Shielding Methods, Modification, Updating and Input Data Preparation - Volume 5 - Two-Dimensional Discrete Ordinates Transport Technique", WANL-PR-(LL)-034, August 1970.

2. Collier, G., et al, "Second Version of the GAMBIT Code", WANL-TME-1969, November 1969.

3. Soltesz, R. G., et al, "Nuclear Rocket Shielding Methods, Modification, Updating and Input Data Preparation - Volume 3, Cross-Section Generation and Data Processing Techniques", WANL-PR-(LL)-034, August 1970.

4. Soltesz, R. G., et al, "Nuclear Rocket Shielding Methods, Modification, Updating and Input Data Preparation - Volume 4 - One-Dimensional Discrete Ordinates Transport Technique", WANL-PR-(LL)-034, August 1970.

5. Anderson, S.L., "Analysis of Neutron Flux Levels and Surveillance Capsule Lead Factors for The Indian Point Unit 2 Reactor", July 1979.

TABLE 1

21 GROUP ENERGY STRUCTURE

GROUP	LOWER ENERGY (MeV)
1	7.79*
2	6.07
3	4.72
4	3.68
5	2.87
6	2.23
7	1.74
8	1.35
9	1.05
10	0.821
11	0.388
12	0.111
13	4.09×10^{-2}
14	1.50×10^{-2}
15	5.53×10^{-3}
16	5.83×10^{-4}
17	7.89×10^{-5}
18	1.07×10^{-5}
19	1.86×10^{-6}
20	3.00×10^{-7}
21	0.0

*Upper energy of group 1 is 10.0 MeV

Table 2

LEAD FACTORS FOR INDIAN POINT UNIT 2

SURVEILLANCE CAPSULES

Capsule Location	Design Basis	L^3P Basis
4° (U, V, W, X)	1.09	1.62
40° (S, T, Y, Z)	3.72	3.48

Table 3

RELATIVE NEUTRON FLUX SPECTRUM AT THE CENTER OF THE SURVEILLANCE CAPSULES

	Relative Neutron Flux			
	Design Basis		L^3P Basis	
Group	4° Capsules	40° Capsules	4° Capsules	40° Capsules
1	.00163	.00852	.00199	.00101
2	.00552	.00283	.00685	.00346
3	.00743	.00447	.00897	.00522
4	.00672	.00467	.00801	.00533
5	.0103	.00793	.0109	.00813
6	.0109	.0155	.0200	.0158
7	.0255	.0219	.0243	.0203
8	.0332	.0299	.0297	.0261
9	.0403	.0373	.0317	.0286
10	.0406	.0382	.0310	.0283
11	.125	.122	.0919	.0882
12	.141	.144	.107	.106
13	.0564	.0586	.0503	.0508
14	.0420	.0438	.0407	.0415
15	.0311	.0326	.0333	.0341
16	.0750	.0800	.0757	.0788
17	.0560	.0595	.0640	.0673
18	.0607	.0661	.0656	.0698
19	.0466	.0508	.0537	.0577
20	.0489	.0530	.0618	.0668
21	.126	.126	.185	.196
ϕ Total	1.30×10^{11}	5.34×10^{11}	1.15×10^{11}	3.08×10^{11}

TABLE 4

REACTION CROSS-SECTIONS FOR ANALYSIS OF FAST NEUTRON MONITORS

		$\sigma(E)$ barns		
GROUP		$Fe^{54}(n,P)Mn^{54}$	$Ni^{58}(n,P)Co^{58}$	$Cu^{63}(n,\alpha)Co^{60}$
1		.592	.607	.035
2		.572	.608	.0098
3		.464	.535	.00085
4		.325	.388	0.0
5		.145	.222	0.0
6		.0494	.113	0.0
7		.0194	.0371	0.0
8		.0089	.0112	0.0
9		.0015	.0043	0.0
10-21		0.0	0.0	0.0
Design Basis	$\bar{\sigma}(4°)$	.087	.113	.000785
	$\bar{\sigma}(40°)$	.067	.0899	.000490
L^3P Basis	$\sigma(4°)$	.106	.136	.00101
	$\sigma(40°)$	.082	.108	.000650

Table 5

SUMMARY OF NEUTRON FLUX MONITOR SATURATED ACTIVITIES
AT THE CENTER OF 2-LOOP PLANT SURVEILLANCE CAPSULES - 1520 MWt

PLANT/CAPSULE	MONITOR ACTIVITY (DPS/gm) $Fe^{54}(n,p)Mn^{54}$	$Ni^{58}(n,p)Co^{58}$	$Np^{237}(n,f)Cs^{137}$	$U^{238}(n,f)Cs^{137}$
A/V	4.53×10^6	5.32×10^7	6.50×10^7	6.37×10^6
A/R	5.53×10^6	8.26×10^7	6.41×10^7	8.51×10^6
B/V	5.28×10^6	8.67×10^7		6.13×10^6
B/R	4.85×10^6	6.26×10^7	7.23×10^7	7.35×10^6
C/V	4.67×10^6	6.84×10^7	5.63×10^7	7.31×10^6
D/V	5.18×10^6	8.04×10^7	7.26×10^7	8.46×10^6
E/V	4.88×10^6	6.70×10^7	7.22×10^7	8.19×10^6
E/R	3.47×10^6	7.83×10^7		7.67×10^6
F/V	5.28×10^6	6.16×10^7	6.58×10^7	9.29×10^6
F/R	4.86×10^6	7.86×10^7	6.79×10^7	9.03×10^6
MEASURED AVERAGE	4.85×10^6	7.19×10^7	6.70×10^7	7.83×10^6
MEASURED MAX./MIN.	1.59	1.63	1.29	1.52
CALCULATED	5.20×10^6	7.70×10^7	6.45×10^7	7.10×10^{96}
CALC./MEAS. AVG.	1.07	1.07	0.96	0.91

Table 6

SUMMARY OF NEUTRON FLUX MONITOR SATURATED ACTIVITIES

AT THE CENTER OF 4-LOOP PLANT SURVEILLANCE CAPSULES - 3565 MWt

PLANT/CAPSULE	MONITOR ACTIVITY (DPS/gm)			
	Fe^{54} (n,p) Mn^{54}	Ni^{58} (n,p) Co^{58}	Np^{237} (n,f) CS^{137}	U^{238} (n,f) Cs^{137}
G/T	4.10×10^6	5.57×10^7		
H/T	3.25×10^6	4.97×10^7		
H/Y	3.95×10^6	5.53×10^7		
I/T	3.26×10^6	4.88×10^7		
J/T	3.54×10^6	5.75×10^7		
K/T	3.62×10^6	4.99×10^7	3.50×10^7	4.69×10^6
K/U	3.69×10^6	4.70×10^7	4.09×10^7	5.61×10^6
L/U	3.50×10^6	5.02×10^7	3.01×10^7	4.02×10^6
MEASURED AVERAGE	3.61×10^6	5.17×10^7	3.54×10^7	4.78×10^6
MEASURED MAX./MIN.	1.26	1.22	1.36	1.40
CALCULATED	3.71×10^6	5.40×10^7	3.87×10^7	4.71×10^6
CALC./MEAS. AVG.	1.03	1.04	1.09	0.99

Table 7

SUMMARY OF $Fe^{54}(n,p)\ MN^{54}$ SATURATED ACTIVITIES
EXTERNAL TO THE REACTOR PRESSURE VESSEL

PLANT/LOCATION	Fe^{54} (n,p) Mn^{54} ACTIVITY (DPS/gm) MEASURED	CALCULATED	CALC./MEAS.
3 LOOP/0°	2.85×10^4	2.48×10^4	0.87
3 LOOP/15°	1.61×10^4	1.82×10^4	1.13
3 LOOP/30°	1.00×10^4	9.60×10^3	0.96
3 LOOP/45°	7.15×10^3	7.10×10^3	0.99
4 LOOP/45°	8.00×10^3	8.25×10^3	1.03

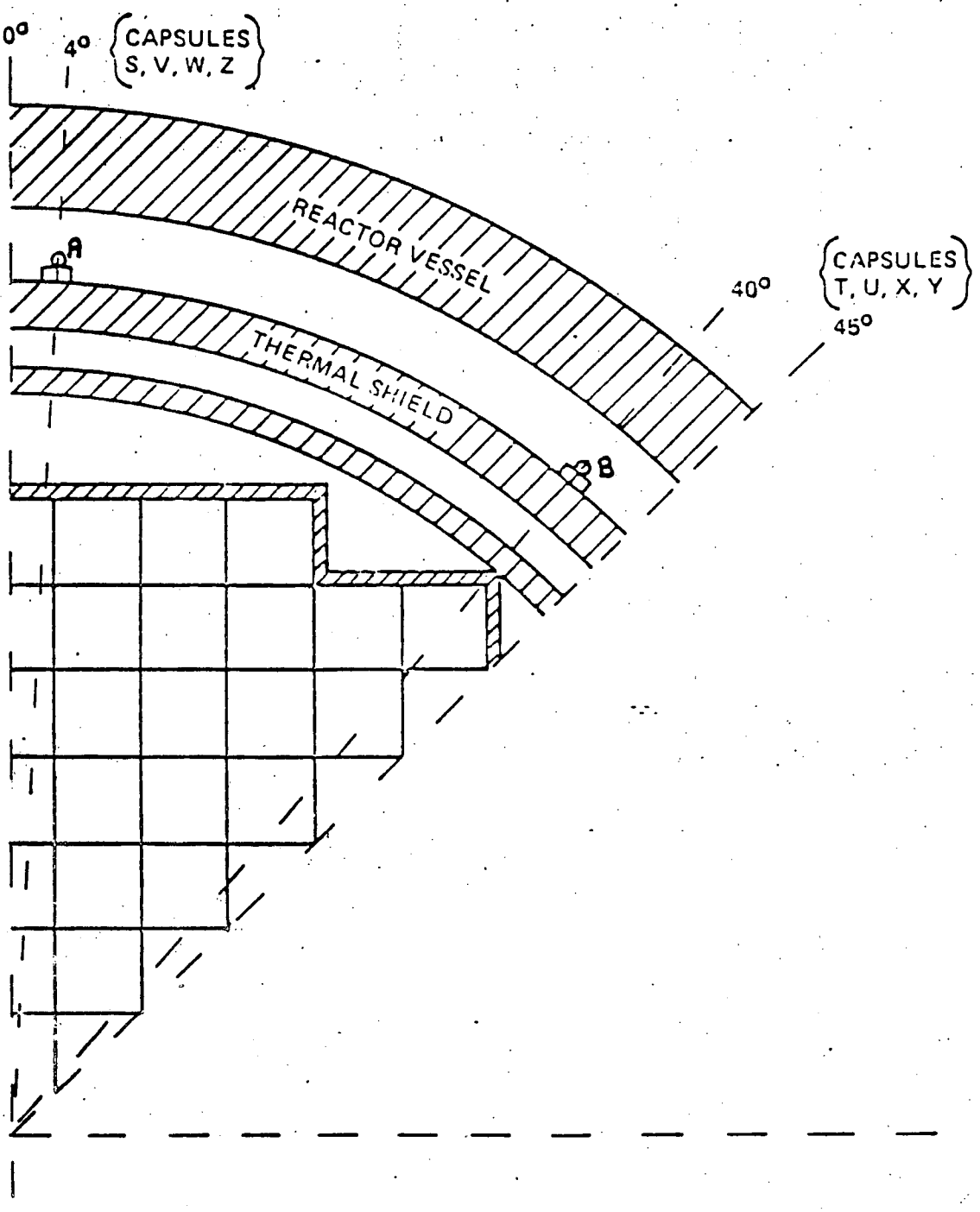

Figure 1
R, Theta Reactor Geometry

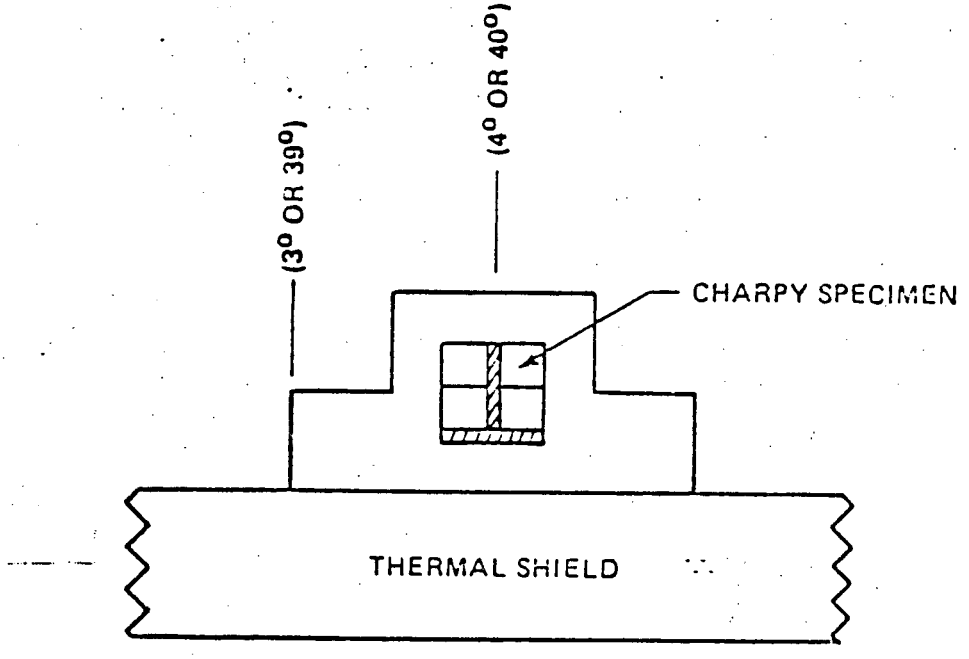

Figure 2
Surveillance Capsule Geometry

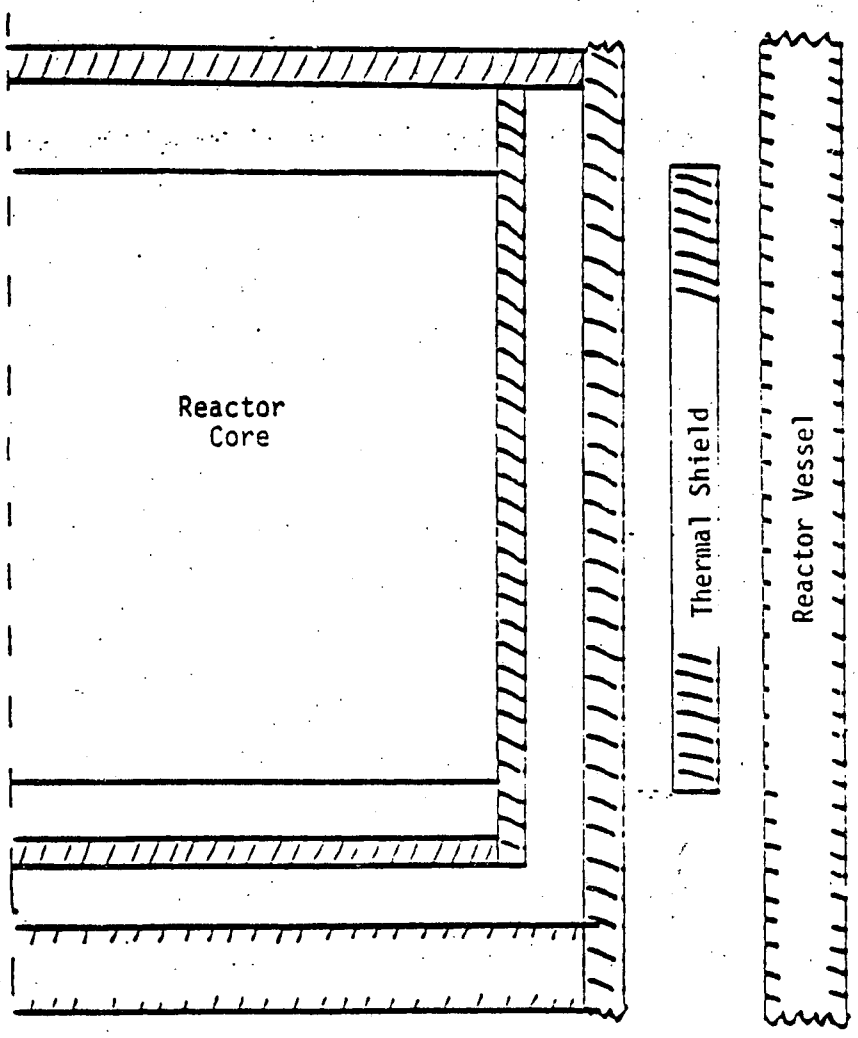

Figure 3
R, Z Reactor Geometry

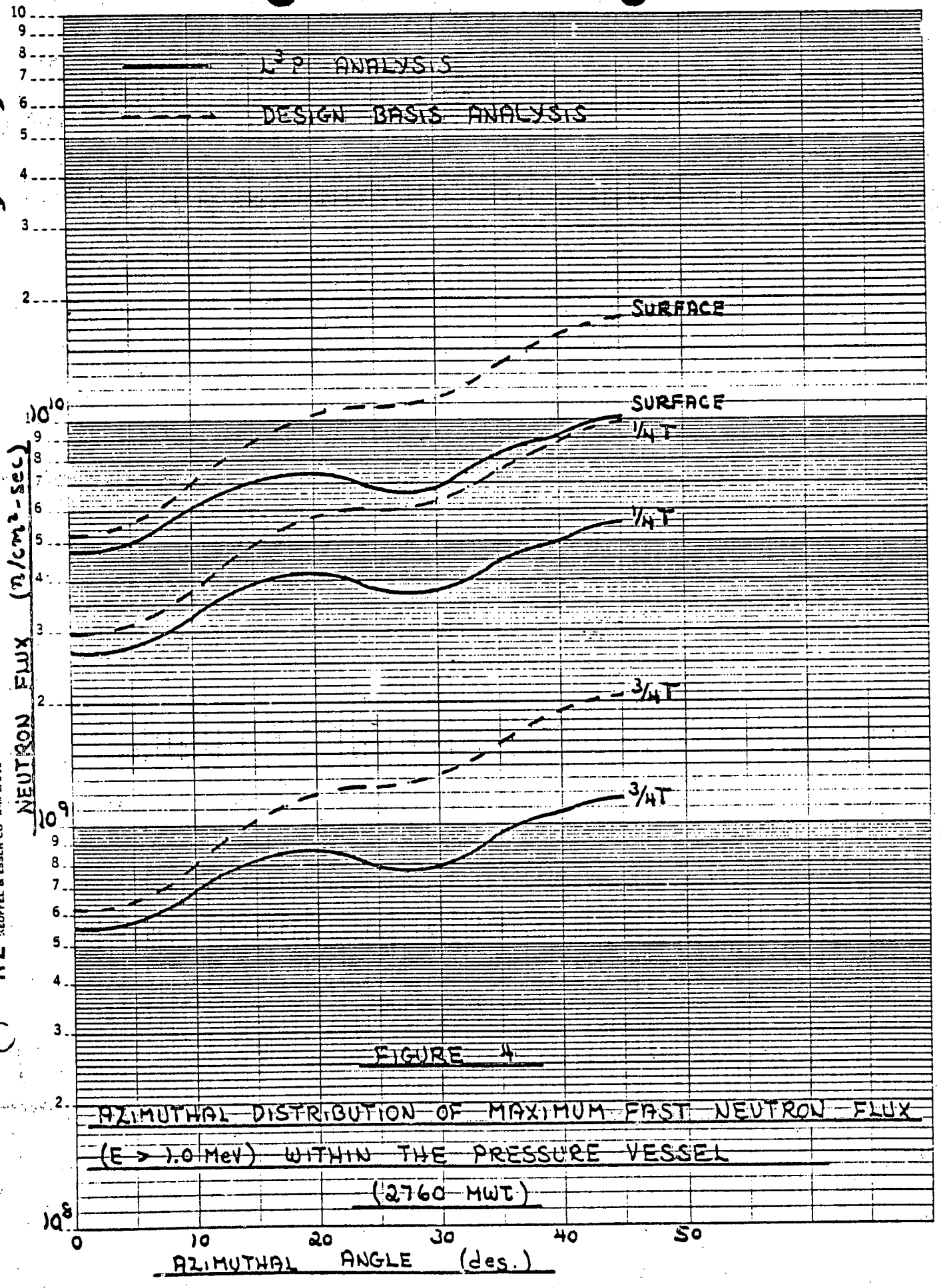

FIGURE 4

AZIMUTHAL DISTRIBUTION OF MAXIMUM FAST NEUTRON FLUX (E > 1.0 MeV) WITHIN THE PRESSURE VESSEL (2760 MWT)

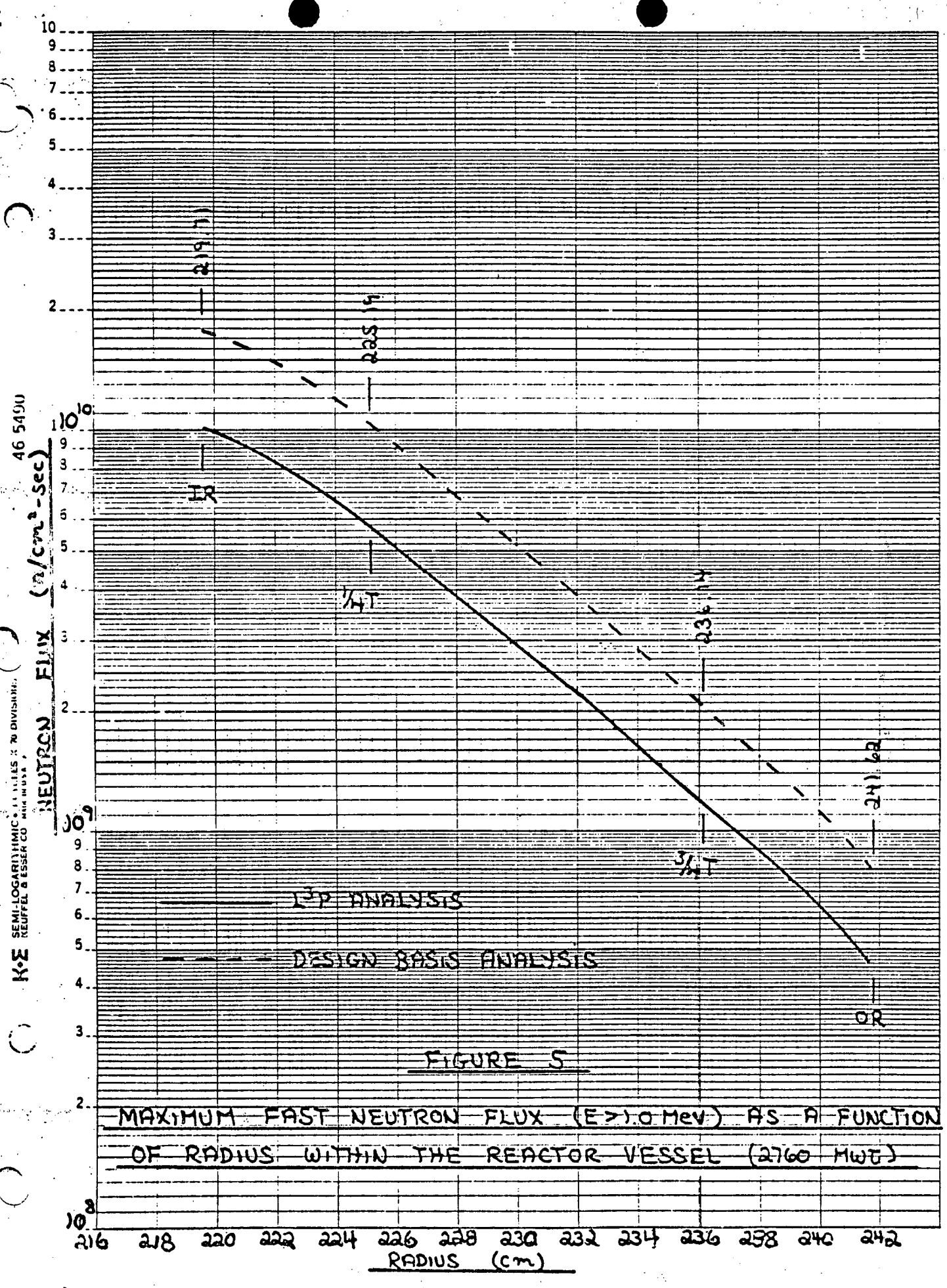

FIGURE 5

MAXIMUM FAST NEUTRON FLUX (E>1.0 MeV) AS A FUNCTION OF RADIUS WITHIN THE REACTOR VESSEL (2760 MWT)

FIGURE 6

RELATIVE AXIAL VARIATION OF FAST NEUTRON FLUX

(E > 1.0 MeV) WITHIN THE REACTOR VESSEL

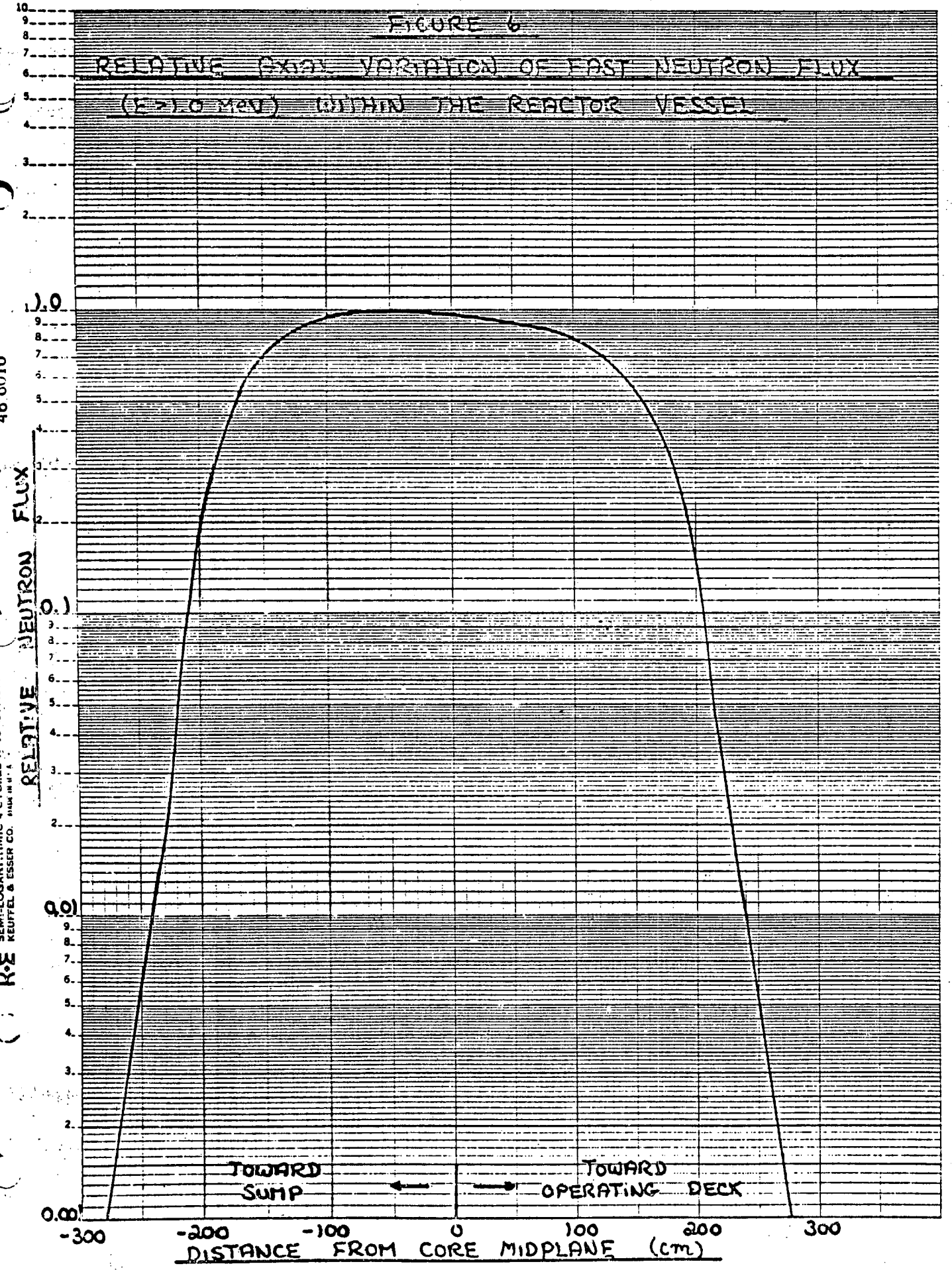

46 6010

K·E SEMI-LOGARITHMIC 4 CYCLES X 70 DIVISIONS
KEUFFEL & ESSER CO. MADE IN U.S.A.

FIGURE 7

AZIMUTHAL VERIATION OF FAST NEUTRON FLUX (E>1.0MeV) THROUGH THE SURVEILLANCE CAPSULE CENTER (2760 MWt)

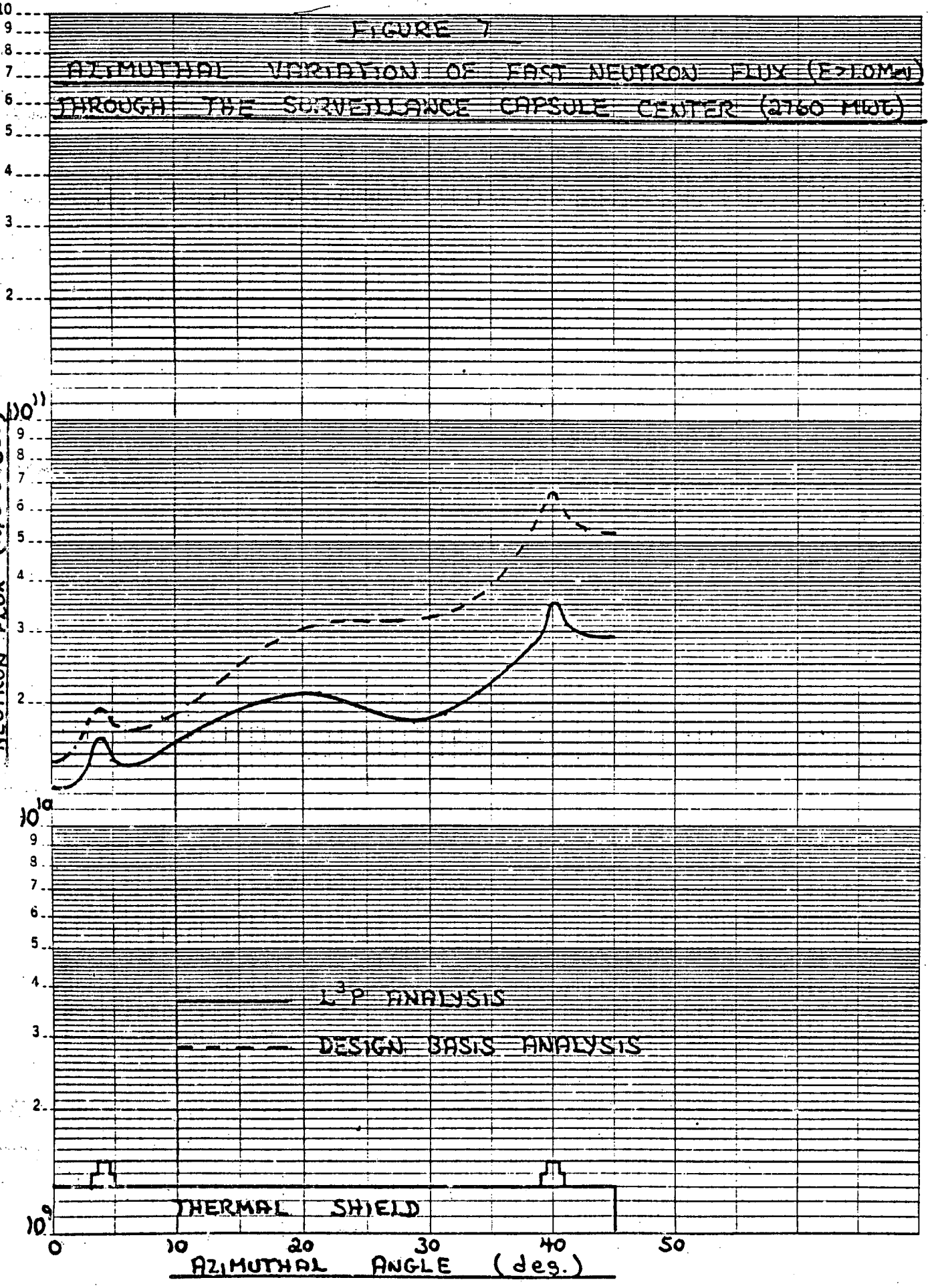

FIGURE 8

RADIAL VARIATION OF FAST NEUTRON FLUX (E > 1.0 MeV) ON THE CORE MIDPLANE WITHIN THE SURVEILLANCE CAPSULES (2760 MWT)